Histol Histopathol (2024) 39: 1659-1667

Histology and Histopathology
From Cell Biology to Tissue Engineering

ORIGINAL ARTICLE Open Access

Correlation of NAT10 expression with clinical data and survival profiles in esophageal squamous cell carcinoma patients, and its impact on cell proliferation and apoptosis

Wei Sun[1,2*], Xiaoying Shen[3*], Xinyi Wang[1,2], Xiaoyan Zhang[3], Yongling Ji[1,2] and Jin Wang[1,2]

[1]Zhejiang Cancer Hospital, Hangzhou, [2]Hangzhou Institute of Medicine (HIM), Chinese Academy of Sciences, Hangzhou, Zhejiang and [3]Shanghai OUTDO Biotech Co. Ltd., Shanghai, China

*These authors contributed equally

Summary. Background. This study investigates the association between NAT10 expression and clinical parameters while assessing prognostic outcomes in esophageal squamous cell carcinoma (ESCC) patients. Furthermore, the study seeks to elucidate the functional role of NAT10 in neoplastic cell proliferation and apoptosis.

Materials and methods. NAT10 expression was assessed in ESCC tissue microarrays through immunohistochemistry (IHC) tests. We employed SPSS software to analyze the correlation between NAT10 staining data, clinical indicators, and their implications for patient prognosis. Small interference RNA (siRNA) was utilized to inhibit NAT10 expression in two esophageal cancer cell lines, TE-1 and KYSE150. Subsequently, we meticulously quantified and compared cellular proliferation and apoptotic ratios among experimental groups. NAT10, Ki67, and Caspase3 expression levels in different groups were evaluated using quantitative polymerase chain reaction (qPCR) and Western blot (WB) assays. Statistical analyses were conducted using GraphPad Prism software, with significance at $P>0.05$.

Results. Our findings indicate that NAT10 is overexpressed in ESCC tissues and exhibits a significant correlation with tumor diameter and overall patient survival. Decreasing NAT10 expression led to the inhibition of tumor cell proliferation and the promotion of apoptosis. Furthermore, siRNA-mediated NAT10 inhibition resulted in the downregulation of Ki67 expression and the concomitant upregulation of Caspase3.

Conclusion. The observed overexpression of NAT10 in ESCC tissues is associated with larger tumor diameters and reduced patient survival. NAT10 appears to play a pivotal role in the progression of esophageal cancer by influencing cell proliferation and apoptosis. These findings suggest potential clinical implications, with Ki67 and Caspase3 potentially participating in this intricate molecular biological process.

Key words: N-acetyltransferase 10 (NAT10), Esophageal squamous cell carcinoma (ESCC), Clinical information, Immunohistochemistry (IHC), siRNA transfection

Corresponding Author: Jin Wang, Hangzhou Institute of Medicine (HIM), Chinese Academy of Sciences, Hangzhou, Zhejiang 310018, China. e-mail: Wangjin@zjcc.org.cn

www.hh.um.es. DOI: 10.14670/HH-18-752

Introduction

Esophageal squamous cell carcinoma (ESCC) is a prevalent and formidable malignancy in the Chinese population, characterized by its high incidence and alarmingly low survival rates (Bray et al., 2018). The grave clinical outlook for ESCC patients underscores the importance of identifying robust prognostic markers and advocating the development of targeted therapeutic strategies within the scientific community.

Abbreviations. AML, Acute Myeloid Leukemia; BCA, Bicinchoninic Acid; cDNA, Complementary DNA; CDK, Cyclin-Dependent Kinase; CCK-8, Cell Counting Kit-8; DMEM, Dulbecco's Modified Eagle Medium; DNA, Deoxyribonucleic Acid; EDTA, Ethylenediaminetetraacetic Acid; ESCC, Esophageal Squamous Cell Carcinoma; GAPDH, Glyceraldehyde-3-Phosphate Dehydrogenase; HNSCC, Head and Neck Squamous Cell Carcinoma; IHC, Immunohistochemistry; NAT10, N-acetyltransferase 10; OD, Optical Density; PBST, Phosphate-Buffered Saline with Tween; PI, Propidium Iodide; PVDF, Polyvinylidene Fluoride; qPCR, Quantitative Polymerase Chain Reaction; RNA, Ribonucleic Acid; RNA-seq, RNA Sequencing; siRNA, Small Interference RNA; WB, Western Blot

N-acetyltransferase 10 (NAT10), an intriguing nuclear entity boasting acetyltransferase and tRNA binding domains, orchestrates a multifaceted repertoire of acetylation processes encompassing histones, microtubules, tRNA, mRNA, and a myriad of other molecular substrates. Beyond these roles, NAT10 assumes a pivotal position in the intricate choreography of cellular mitosis and the orchestration of stress response mechanisms, culminating in its distinctive overexpression across a diverse spectrum of neoplastic tissues (Lv et al., 2003; Liu et al., 2007; Shen et al., 2009; Ito et al., 2014; Arango et al., 2018).

The extant body of scientific literature has borne witness to an array of investigations scrutinizing the correlation between NAT10 and various malignancies, uncovering aberrant expression profiles within cancerous tissues. These endeavors have illuminated NAT10's potential as a prognostic determinant (Han et al., 2018; Tan et al., 2018; Zhang et al., 2018; Ma et al., 2022) and a contributory factor to drug resistance among patients grappling with cancer (Wu et al., 2018; Zhang et al., 2019; Qi et al., 2022). Nevertheless, a conspicuous gap in the existing literature persists, as no prior investigations have probed the relationship between NAT10 and ESCC. Consequently, the present study embarks on a dedicated exploration to elucidate the nuanced functional landscape of NAT10 within the context of ESCC. The ensuing revelations bring to light a significant nexus between heightened NAT10 expression and ameliorated tumor dimensions, offering a ray of hope for improved prognoses among afflicted individuals. Furthermore, a meticulous dissection of *in vitro* cytological dynamics buttresses the premise that NAT10 inhibition may serve as a compelling intervention, impeding tumor cell proliferation, fostering apoptosis, and concurrently modulating the expression levels of Ki67 and CASP3.

Materials and methods

Study materials

The investigation utilized an ESCC cDNA array (MecDNA-HEsoS030PG01), comprising 30 cDNA spots from 15 patients, and a tissue microarray (HEsoS180Su08), housing 114 ESCC tissues and 66 matched adjacent tissues, all procured from Shanghai OUTDO Biotech Co. Ltd. (Shanghai, China). The ESCC tissue microarray specimens were meticulously annotated with pertinent patient demographic and clinical data, including gender, age, tumor diameter, pathological grade, T stage, lymph node metastasis, distant metastasis, and clinical stage (Table 1). The sample acquisition spanned April 2006 to December 2008, and a five-year comprehensive patient follow-up exceeding five years concluded in June 2015. Notably, the tissue samples employed in this study were obtained exclusively from ESCC surgical procedures, ensuring the exclusion of any prior radiotherapy, chemotherapy, or targeted therapeutic interventions. Ethical endorsement for this research was secured from the Ethics Committee of Shanghai OUTDO Biotech Co. Ltd.

RNA extraction and real-time quantitative polymerase chain reaction (qPCR)

Total RNA extraction from cells employed Trizol reagents (Sigma, Missouri, USA, Cat. T9424-200ml). The purity of RNA was assessed employing an Ultraviolet spectrophotometer (NanoDrop, Wilmington, USA, Cat. ND-1000), while RNA quality was ascertained via Lab on a chip (Agilent, Santa Clara, USA, Cat. Agilent 2100). Subsequently, cDNA synthesis was achieved using SuperScript IV Reverse Transcriptase (Thermo Fisher, MA, USA, Cat. 18090010).

The qPCR experiments were meticulously executed to quantify the mRNA expression levels of NAT10,

Table 1. The relationship between NAT10 expression and the clinical characteristics in ESCC patients was analyzed by a chi-square test.

Clinical characteristics	Total samples (n=95)	NAT10 low expression (n=60)	NAT10 high expression (n=35)	Chi-square value	*P*-value
Gender				3.537	0.060
Male	71	41	30		
Female	24	19	5		
Age (years)				7.083	0.008**
≤60	26	22	4		
>60	69	38	31		
Tumor diameter (cm)				5.325	0.021*
≤5 cm	59	32	27		
>5 cm	36	28	8		
Pathological Grade				4.096	0.129
Grade 1	4	4	0		
Grade 2	69	45	24		
Grade 3	22	11	11		
T stage				0.530	0.912
T1	4	2	2		
T2	15	10	5		
T3	74	47	27		
T4	2	1	1		
Lymph node metastasis				0.032	0.858
Negative	45	28	17		
Positive	50	32	18		
Distant metastasis				NA	NA
Negative	95	60	35		
Positive	0	0	0		
Clinical stage				1.034	0.596
Clinical stage 1	4	2	2		
Clinical stage 2	44	30	14		
Clinical stage 3	47	28	19		
Clinical stage 4	0	0	0		

*, $P<0.05$; **, $P<0.01$. NAT10, N-acetyltransferase 10; ESCC, esophageal squamous cell carcinoma. Grade 1, good differentiation; Grade 2, moderate differentiation; Grade 3, poor differentiation. cm, centimeter; NA, no answer.

Ki67, and Caspase3, with Beta-Actin as the internal reference control. Primer sequences were as follows: NAT10 forward primer: 5'-GCCTCTTGTAAGAAGT GTCTCG -3', Reverse primer: 5'-TCTTTTCAGAGATG CCCTCGAT-3'; Ki67 forward primer: 5'-CCTGCTCGA CCCTACAGAGTG-3', Reverse primer: 5'- GTTGC TCCTTCACTGGGGTC-3'; Caspase3 forward primer: 5'-GGTTCATCCAGTCGCTTTG-3', Reverse primer: 5'-ATTCTGTTGCCACCTTTCGG-3'; Beta-Actin forward primer: 5'-GAAGAGCTACGAGCTGCCTGA-3', Reverse primer: 5'-CAGACAGCACTGTGTTG GCG-3'. The qPCR protocol consisted of an initial denaturation at 95°C for 25 seconds, followed by denaturation at 95°C for 5 seconds, annealing at 60°C for 30 seconds, and a total of 35 cycles. Fluorescence signals were detected during the extension step at 60°C, and fluorescence data were systematically collected from 60 to 90°C. Gene-specific primers were synthesized by ShengGong (Shanghai, China), and the qPCR reaction was conducted employing the SYBR Green premix Ex-Taq qPCR™ II kit (TAKARA, Osaka, Japan, Cat. RR820Q).

Table 2. The univariate analysis of overall survival time in ESCC was performed by the Kaplan-Meier method and log-rank test.

Variables	Total samples (n=95)	Mean OS (months)	log-rank (Chi-Square)	*P*-value
NAT10 expression group			5.395	0.020*
NAT10 low expression	60	38.47±4.54		
NAT10 high expression	35	23.37±3.72		
Gender			8.156	0.004**
Male	71	27.28±3.28		
Female	24	49.54±7.62		
Age (years)			0.204	0.652
≤60	26	34.92±6.31		
>60	69	32.14±3.81		
Tumor diameter (cm)			6.654	<0.010**
≤5 cm	59	38.80±4.29		
>5 cm	36	23.25±4.54		
Pathological Grade			1.458	0.483
Grade 1	4	35.75±19.29		
Grade 2	69	30.38±3.73		
Grade 3	22	40.32±7.05		
T stage			12.340	0.006**
T1	4	74.50±6.51		
T2	15	52.80±8.40		
T3	74	26.49±3.39		
T4	2	38.00±20.00		
Lymph node metastasis			9.559	0.002**
Negative	45	44.22±5.15		
Positive	50	22.72±3.55		
Distant metastasis			NA	NA
Negative	95	_		
Positive	0	_		
Clinical stage			25.844	< 0.001***
Clinical stage 1	4	74.50±6.51		
Clinical stage 2	44	45.55±5.32		
Clinical stage 3	47	17.53±2.66		
Clinical stage 4	0	_		

*, *P*<0.05; **, *P*<0.01, ***, *P*<0.001. NAT10, N-Acetyltransferase 10; OS, overall survival time; Grade 1, good differentiation; Grade 2, moderate differentiation; Grade 3, poor differentiation. cm, centimeter; NA, no answer.

Immunohistochemistry (IHC)

An IHC assessment was performed on the tissue microarray specimens, following a methodical protocol. This encompassed dewaxing and antigen retrieval employing EDTA solution (Double-helix, N61111). Subsequently, primary antibody anti-NAT10 (1:500, Abcam, Cambridge, UK, Cat. Ab1194297) was meticulously applied and incubated overnight at 4°C. A secondary antibody (instant, EnVision FLEX/HRP, DAKO, Copenhagen, Denmark, Cat. SM802) was subsequently introduced and incubated at room temperature for 25 minutes. Sections were carefully washed with PBST buffer solution (DAKO, Copenhagen, Denmark, Cat. DM831) and stained with DAB (DAKO, Copenhagen, Cat. DM827).

The IHC staining score for NAT10 was meticulously evaluated by expert pathologists, employing a comprehensive scoring system. Staining percentage was graded as 0 (no staining), 1 (1-20% staining), 2 (21-40% staining), 3 (41-60% staining), 4 (61-80% staining), and 5 (81-100% staining). Simultaneously, staining intensity was recorded as 0 (no staining), 1 (weak staining), 2 (moderate staining), and 3 (intense staining). The final IHC score was calculated by multiplying the percentage and intensity scores.

Table 3. The independent survival factors of overall survival time in ESCC were analyzed by the Cox multivariate regression method.

	B	SE	Wald	df	Sig.	Exp(B)	95.0% CI for Exp(B)	
							Lower	Upper
NAT10 expression	0.625	0.258	5.875	1	0.015*	1.867	1.127	3.094
Gender	-0.492	0.329	2.232	1	0.135	0.611	0.321	1.166
Tumor diameter	0.736	0.249	8.742	1	0.003**	2.088	1.282	3.402
T stage	0.645	0.227	8.063	1	0.005**	1.906	1.221	2.975
Lymph node metastasis	0.565	0.249	5.144	1	0.023*	1.759	1.080	2.865

*, *P*<0.05; **, *P*<0.01; ***, *P*<0.001. NAT10, N-acetyltransferase 10.

Western blot assay (WB)

For the WB analysis, cells were treated with pre-cooled RIPA lysis buffer (Beyotime, Nanjing, China, Cat. P0013B) for 15 minutes, followed by centrifugation at 12,000 rpm for 20 minutes. The supernatant was collected, and protein concentration was quantified using the BCA method. The protein samples were separated by 10% sodium dodecyl sulfate-polyacrylamide gel electrophoresis (SDS-PAGE) using Beyotime kits (Nanjing, China, Cat. P0012A, P0014B). Subsequently, the separated proteins were transferred onto a polyvinylidene fluoride (PVDF) membrane (Millipore, Massachusetts, USA, Cat. IPFL00010).

The PVDF membrane was blocked with a 5% milk-blocking solution before being incubated overnight at 4°C with primary antibodies against NAT10 (1:2000, Abcam, Cambridge, UK, Cat. Ab1194297), Ki67 (1:1000, Proteintech, Wuhan, China, Cat. 28074-1-AP), and Caspase3 (1:2000, Proteintech, Wuhan, China, Cat. 66470-2-Ig). Subsequently, a secondary antibody was applied and incubated for 30 minutes, followed by alkaline phosphatase (ALP) staining. GAPDH was utilized as the loading control.

Cell culture and transfection

ESCC cell lines TE-1 and KYSE150, procured from the Chinese Academy of Sciences (Shanghai, China, Cat. TCHu232) and authenticated through karyotype analysis, were cultured in DMEM medium (Gibco, NY, USA, Cat. 12430054) supplemented with 10% fetal bovine serum (Gibco, NY, USA, Cat. 10099141C) at 37°C until reaching the logarithmic growth phase. Subsequently, cells were adjusted to 30,000-50,000 cells/ml density and incubated at 37°C for 24 hours. Following a PBS wash (Thermo Fisher, MA, USA, Cat. 10010049), cells were resuspended in a serum-free medium (Gibco, NY, USA, Cat. 12430054).

Transfection was accomplished using Lipofectamine 2000 (Thermo Fisher, MA, USA, Cat. 11668019), and siRNA (GenePharma, Shanghai, China, Cat. A10001) was introduced into the cells. The siRNA sequence was as follows: sense chain 5'GGCCAAAGCUGU CUGAAATT3' and antisense chain 5'UUUUCAAGA CAGCUUUGGCCTT3'. The cells were categorized into a control group (transfected with siRNA-NC) and an experimental group (transfected with siRNA-NAT10). After 24 hours of transfection, cells were adjusted to the appropriate density and seeded in various-sized well plates for subsequent cell proliferation and apoptosis analysis.

Cell proliferation test

Cells, adjusted to a concentration of 50 cells/μl, were transfected for 24 hours. Post-transfection, cells were plated in 96-well plates at a density of 100 μl per well and incubated at 37°C for 24 hours. Subsequently, ten μl of CCK8 reagent (Vazyme, Nanjing, China, Cat. A311-01) was added to each well and incubated at 37°C for 1 hour. The absorbance (OD value) was measured at 450 nm using an enzyme-labeled instrument (Allsheng, Hangzhou, China, Cat. ARM-100). The cell proliferation rate was calculated as follows:

Cell Proliferation Rate = (OD value of experimental group - OD value of blank group) / (OD value of control group - OD value of blank group) × 100%.

Cell apoptosis assay

Following a 24-hour transfection period, cells were enzymatically detached and resuspended in a culture medium. Cell concentration was standardized to 50 cells/μl, and 100 μl of the cell suspension was seeded into each well of a 96-well plate. The cells were subsequently incubated at 37°C for an additional 24 hours.

Subsequently, 100 μl of staining solution containing Hoechst (10 μg/ml) and PI (20 μM) (Beyotime, Nanjing, China, Cat. C1052) was added to each well. The cells were cultured at 37°C for 20 minutes without light. Finally, the staining results of the cells were analyzed utilizing the ACUMEN instrument (TTP Labtech, Cambridge, UK, Cat. Acumen eX3).

Statistical analysis

Statistical analysis was conducted employing SPSS 17.0 software (IBM Corporation, Armonk, NY, USA). The IHC staining data were scrutinized for associations with clinical features using the paired t-test to ascertain differences in NAT10 expression between cancerous and paracancerous tissues. Additionally, the relationship between NAT10 expression and clinical characteristics in ESCC was assessed via the Chi-square test.

Univariate analysis of overall survival was performed utilizing Kaplan-Meier and log-rank tests. Variables exhibiting statistical significance were subsequently incorporated into a Cox multivariate regression survival analysis. Furthermore, data from the cell proliferation and apoptosis assays and qPCR results were analyzed using GraphPad Prism 7.0 Software (GraphPad Software, Inc, La Jolla, CA, USA). A significance level of $P<0.05$ was deemed statistically significant.

Results

NAT10 overexpression in ESCC tissues

NAT10 exhibited significant overexpression within ESCC tissues. The mRNA expression of NAT10 in the ESCC cDNA array was assessed via qPCR, and subsequent data analysis utilizing the paired t-test revealed noteworthy findings. Specifically, NAT10 mRNA expression levels in the 15 cancer tissues were markedly higher when compared with their correspond-

ing adjacent tissues. Notably, the average expression value of this gene within the cancerous tissues was elevated by 293% (P<0.001) (Fig. 1A).

Additionally, IHC staining assays unveiled the predominant localization of the NAT10 protein within the nucleus (Fig. 1C). Among the analyzed samples, 19 exhibited substantial protein overexpression in the cancerous tissues, while 13 displayed comparatively lower protein expression levels within the same context. Remarkably, no discernible differences were observed in the remaining three paired cancer and adjacent tissues. Furthermore, the paired t-test was conducted to validate the elevated presence of NAT10 protein in esophageal cancer tissues, revealing a modest increase (8.07±0.53 vs. 7.03±0.44, P=0.082), albeit not statistically significant (Fig. 1B).

NAT10 overexpression in ESCC tissues correlates with clinical parameters and prognosis

The overexpression of NAT10 in ESCC tissues exhibited significant associations with a larger tumor diameter and shortened prognostic outcomes. IHC staining data were garnered from 95 cancer tissues and 35 adjacent tissues, excluding exfoliated tissue points observed during experimentation and cases lacking comprehensive pathological data. ESCC patients were stratified into two groups based on NAT10 expression within cancer tissues: the NAT10 low expression group and the NAT10 high expression group, determined by the average total staining score. Within this context, the low expression group comprised 60 cases (total IHC staining score <9), while the high expression group encompassed 35 cases (total staining score >9).

Utilizing the Chi-square test, a correlation analysis was conducted between NAT10 expression and various clinical parameters of patients. This analysis revealed significant associations between NAT10 expression and age and tumor diameter (P=0.008, P=0.021, respectively), while no significant correlations were observed with gender, pathological grade, T stage, lymph node metastasis, distant metastasis, or clinical stage (P>0.05) (Table 1).

Furthermore, univariate survival analysis unveiled a strong link between NAT10 expression and ESCC prognosis. Patients in the NAT10 high expression group

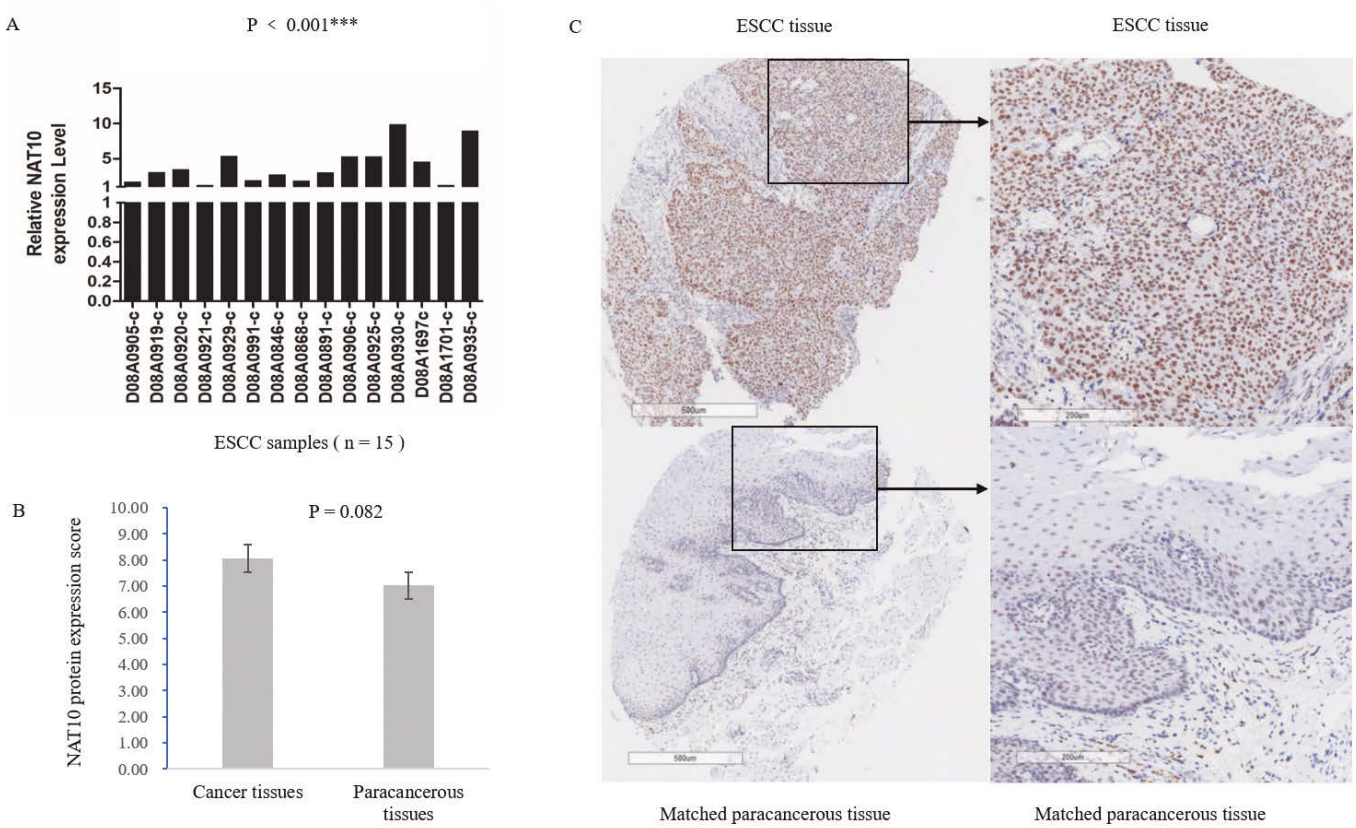

Fig. 1. The expression level of NAT10 in ESCC tissues and the matched paracancerous tissues was detected by qPCR and IHC. **A.** NAT10 mRNA expression in ESCC and the adjacent tissues was tested by qPCR. **B.** NAT10 protein expression in cancer and the paracancerous tissues was assayed by IHC. **C.** NAT10 protein expression level in ESCC and the adjacent tissues was assayed by IHC. ***, P<0.001. NAT10, N-acetyltransferase 10; ESCC, esophageal squamous cell carcinoma; n, number; qPCR, real-time quantitative polymerase chain reaction; IHC, immunohistochemistry.

exhibited significantly shorter overall survival rates compared with their counterparts in the low expression group (23.37±3.72 months vs. 38.47±4.54 months, P=0.020) (Fig. 2). This analysis also identified gender, tumor diameter, T stage, lymph node metastasis, and clinical stage as prognostic factors (P=0.004, P<0.010, P=0.006, P=0.002, P<0.001, respectively).

Finally, Cox multiple regression survival analysis was conducted, encompassing all aforementioned prognostic factors. The results revealed NAT10, tumor size, T stage, and lymph node metastasis as independent predictors (P=0.015, P=0.003, P=0.005, P=0.023, respectively), while gender did not emerge as an independent predictor (P=0.135).

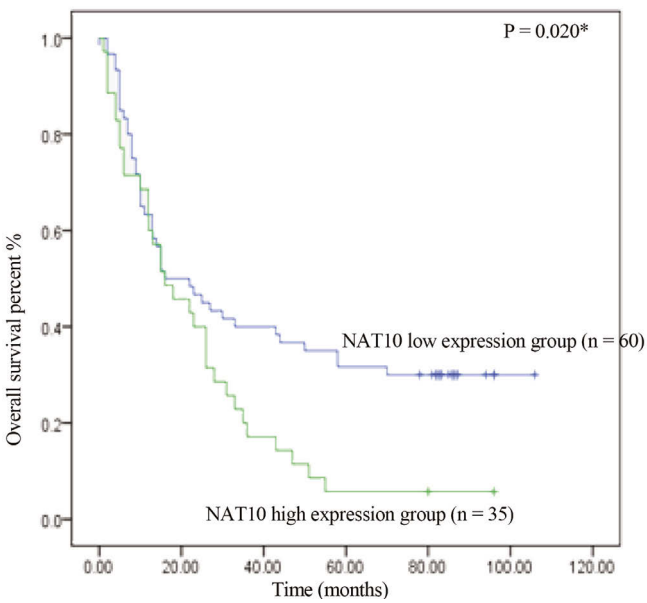

Fig. 2. The association of NAT10 expression with the overall survival of ESCC was analyzed by Kaplan-Meier and Log-rank test. *, P<0.05. NAT10, N-acetyltransferase 10; ESCC, esophageal squamous cell carcinoma; n, number.

Suppression of NAT10 expression impedes ESCC cell proliferation, promotes apoptosis, and modulates Ki67 and Caspase3 Levels

Two ESCC cell lines, TE-1 and KYSE150, were cultured, and siRNA was employed to downregulate NAT10 expression within the cells. Subsequent qPCR assays unveiled a marked reduction in NAT10 expression within TE-1 and KYSE 150 cells transfected with siRNA-NAT10, with reductions of 85.49% and 86.14%, respectively (P<0.001 for both, Fig. 3A), in comparison with control cells transfected with siRNA-NC. Complementing these findings, WB experiments confirmed that siRNA-NAT10 transfection significantly inhibited NAT10 protein expression in ESCC cells (Fig. 3B).

Following a 48-hour transfection period, CCK-8 proliferation tests and Hoechst/PI staining assays were conducted to assess variations in cell proliferation and apoptosis rates within each group. The results demonstrated that TE-1 and Kyse150 cells transfected with siRNA-NAT10 exhibited proliferation rates reduced by 12.43% and 16.37%, respectively (P=0.034, P<0.001) (Fig. 4A), alongside apoptosis rates increased by 58.16% and 26.77%, respectively (P<0.001, P=0.039) (Fig. 4B). Consequently, the suppression of NAT10 expression was associated with a decrease in ESCC cell proliferation and an increase in apoptosis rates.

To elucidate the molecular mechanisms underlying NAT10's influence on esophageal cancer cell function, qPCR and WB methods were employed to assess the expression changes of several genes related to tumor proliferation and apoptosis. The qPCR data indicated that the downregulation of NAT10 expression led to a reduction in Ki67 expression by 22.96% and 46.56% in TE-1 and Kyse150 cells, respectively (P=0.002, P<0.001), while Caspase3 expression increased by 47.71% and 23.43%, respectively (P=0.013, P=0.010) (Fig. 5). WB results for these two proteins aligned with the qPCR data (Fig. 6). Based on these experimental

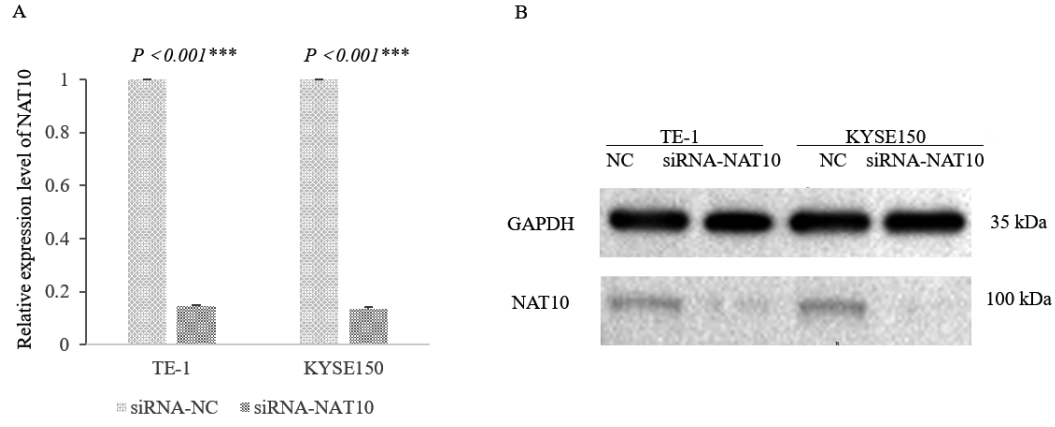

Fig. 3. NAT10 expression change in ESCC cell lines TE-1 and KYSE150 was detected by qPCR **(A)** and WB experiments **(B)** after 48 hours of transfection. ***, P<0.001. NAT10, N-acetyltransferase 10; ESCC, esophageal

findings, it is conjectured that NAT10 may promote cancer cell proliferation and inhibit apoptosis by modulating the expression levels of Ki67 and Caspase3.

Discussion

Our study presents compelling findings regarding NAT10 expression and its implications in ESCC, providing crucial insights into its role as a prognostic marker and potential therapeutic target. We highlight its consistent upregulation in ESCC tissues, predominantly localized within the nucleus, and establish its association with larger tumor diameter and shorter overall survival. Importantly, these findings align with a growing body of literature demonstrating NAT10's tumor-promoting effect across various cancer types.

Prior research has elucidated analogous patterns of NAT10 dysregulation in different malignancies. For instance, studies by Liang et al. (2020) and Zi et al. (2020) uncovered elevated NAT10 expression in acute myeloid leukemia (AML), correlating with poor survival outcomes (Liang et al., 2020; Zi et al., 2020). This aligns with our observations in ESCC, reinforcing NAT10's adverse prognostic implications.

Furthermore, NAT10 has been identified as significantly overexpressed in bladder cancer, non-small cell lung cancer, HNSCC, and several other tumor types, consistently linked to accelerated cancer progression and reduced survival rates. These findings collectively emphasize NAT10's role as a tumor-promoter.

Recent advancements in bladder cancer research have enriched our understanding of NAT10's multifaceted role. Elevated NAT10 expression in bladder cancer corresponds to adverse clinical parameters, including higher pathological grades, lymph node metastasis, advanced tumor stages, and diminished overall survival. Functional experiments involving shRNA-mediated NAT10 inhibition in bladder cancer cell lines (T24 and UMUC-3) demonstrated remarkable reductions in cell proliferation, migration, invasiveness, and increased apoptosis rates. These *in vivo* findings further support NAT10's role, as tumor-bearing mice with NAT10 suppression exhibited reduced tumor burden and growth. Additionally, this study provided insights into the mechanistic underpinnings, revealing NAT10's influence on mRNA modifications and its impact on crucial cancer-related genes, such as *BCL9L*, *SOX4*, and *AKT1*, ultimately fueling cancer progression (Wang et al., 2022a,b).

In our study, we employed siRNA targeting NAT10

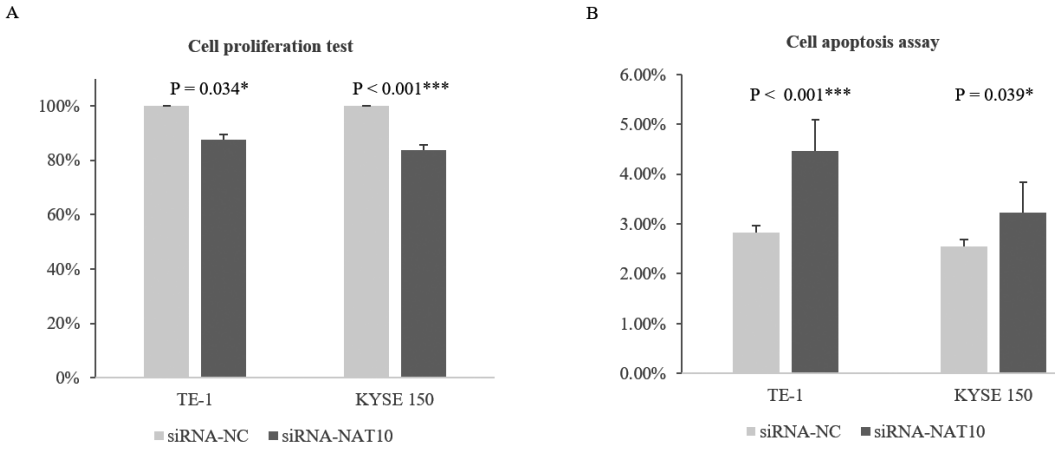

Fig. 4. After 48 hours of transfection, the changes of cell proliferation and apoptosis in each group were detected by CCK8 assay and Hochest / PI staining. *, *P*<0.05; ***, *P*<0.001. NAT10, N-acetyltransferase 10.

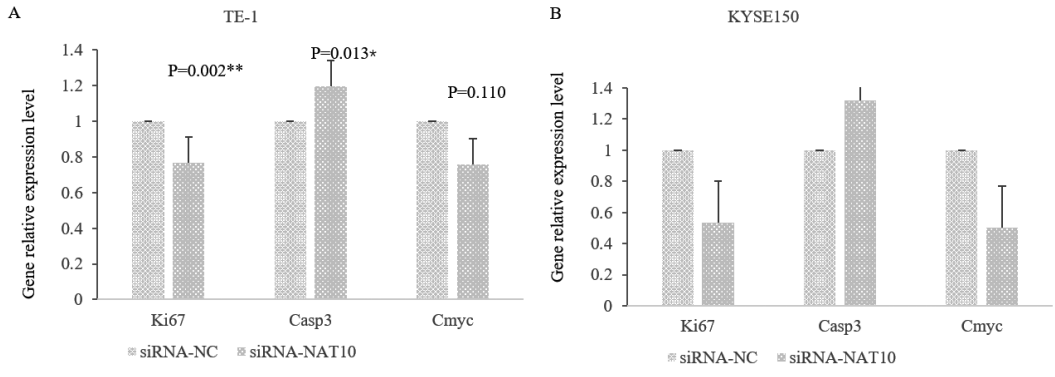

Fig. 5. The mRNA relative expression level of ki67 and Casp3 in different transfected ESCC cell groups were detected by qPCR test. *, *P*<0.05; **, *P*<0.01; ***, *P*<0.001. NAT10, N-acetyltransferase 10; ESCC, esophageal squamous cell carcinoma; qPCR, real-time quantitative polymerase chain reaction; WB, western blot.

to elucidate its effects in ESCC cell lines (TE-1 and KYSE150). Our results reveal that NAT10 down-regulation significantly hampers tumor cell proliferation and promotes apoptosis. This was further substantiated by qPCR and WB analyses, where reduced NAT10 expression concurrently led to suppressed Ki67 (a cell proliferation marker) and elevated Caspase3 (a pro-apoptotic protein) expression. This suggests that NAT10 may orchestrate tumor cell proliferation and apoptosis through its impact on Ki67 and Caspase3 expression, ultimately contributing to ESCC progression (Zi et al., 2020).

Notably, the specific molecular mechanisms driving NAT10's tumor-promoting effects exhibit heterogeneity across different cancers. C-myc has been implicated as a transcription factor mediating NAT10 upregulation, thereby promoting non-small cell lung cancer cell proliferation and migration. Conversely, AML studies demonstrate NAT10's role in inducing cell cycle arrest and activating apoptosis pathways, impacting key regulators such as CDK2, CDK4, CyclinD1, Cyclin E, p16, and p21. NAT10 knockout or inhibition increases apoptotic protein expression (Bax and Bak) while decreasing anti-apoptotic Bcl2 levels, culminating in classic apoptotic pathways.

NAT10's involvement in drug resistance has also been explored. Targeting NAT10 has shown promise in reversing epithelial-mesenchymal transformation and doxorubicin resistance in liver and breast cancer cells (Wu et al., 2018; Zhang et al., 2019). Recent investigations in breast cancer unveiled NAT10's role in oxaliplatin resistance, elucidating a mechanism involving NAT10's interaction with PARP1, resulting in PARP1 acetylation, extended PARP1 half-life, and enhanced recruitment of DNA damage repair-associated proteins. This augments DNA damage repair, promoting breast cancer cell viability and resistance to oxaliplatin (Qi et al., 2022).

In conclusion, our study provides crucial evidence linking aberrant NAT10 expression to tumor size and overall prognosis in ESCC, highlighting its role in driving esophageal squamous cell carcinoma progression. This is mediated, in part, through the regulation of cell proliferation and apoptosis, with the participation of Ki67 and Caspase3. Despite these insights, the intricate regulatory mechanisms governing NAT10 in ESCC remain enigmatic, representing a pivotal area for future research. Further investigations are warranted to unravel the specific molecular pathways driving NAT10's tumor-promoting effects in different cancer contexts and explore its potential as a therapeutic target.

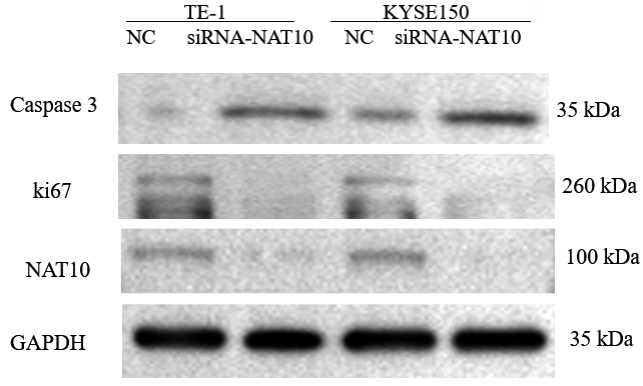

Fig. 6. The protein relative expression level of ki67, Casp3 and NAT10 in different transfected ESCC cell groups were detected by qPCR test. *, $P<0.05$; **, $P<0.01$; ***, $P<0.001$. NAT10, N-acetyltransferase 10; ESCC, esophageal squamous cell carcinoma; qPCR, real-time quantitative polymerase chain reaction; WB, western blot.

Acknowledgements. We thank the patients for their time and participation in this study.

Funding. This work was supported by grants from the Zhejiang province public welfare funds (No. LGF20H160009) and the Medical Science and Technology Project of Zhejiang Province (No. 2021455891).

Conflict of Interest Statement. The authors of this article declare that they have no financial or personal conflicts of interest that could influence the research, data interpretation, or presentation of results. No competing financial interests or relationships with organizations that could directly or potentially impact the work described in this article exist. This includes but is not limited to employment, consultancies, stock ownership, honoraria, and paid expert testimony.

The authors are committed to upholding the highest standards of transparency and integrity in their research and have disclosed any potential conflicts of interest accurately.

If any conflicts of interest arise subsequent to the publication of this article, the authors will promptly provide an update or correction.

References

Arango D., Sturgill D., Alhusaini N., Dillman A.A., Sweet T.J., Hanson G., Hosogane M., Sinclair W.R., Nanan K.K., Mandler M.D., Fox S., Zengeya T.T., Andresson T., Meier J.L., Coller J. and Oberdoerffer S. (2018). Acetylation of Cytidine in mRNA promotes translation efficiency. Cell 175, 1872-1886.

Bray F., Ferlay J., Soerjomataram I., Siegel R.L., Torre L.A. and Jemal A. (2018). Global cancer statistics 2018: GLOBOCAN estimates of incidence and mortality worldwide for 36 cancers in 185 countries. CA Cancer J. 66, 394-424.

Han F., Liu H.Q. and Wang S.Y. (2018). Expression of CD117, MITF, and NAT10 and their prognostic values in sinonasal mucosal melanoma. Zhonghua Bing Li Xue Za Zhi. 47, 931-935 (in Chinese).

Ito S., Horikawa S., Suzuki T., Kawauchi H., Tanaka Y., Suzuki T. and Suzuki T. (2014). Human NAT10 is an ATP-dependent RNA Acetyltransferase responsible for N4-acetylcysteine formation in 18 S ribosomal RNA (rRNA). J. Biol. Chem. 289, 35724-35730.

Liang P., Hu R., Liu Z., Miao M., Jiang H. and Li C. (2020). NAT10 upregulation indicates a poor prognosis in acute myeloid leukemia. Curr. Probl. Cancer 44, 100491.

Liu H., Ling Y., Gong Y., Sun Y., Hou L. and Zhang B. (2007). DNA damage induces N-acetyltransferase NAT10 gene expression

through transcriptional activation. Mol. Cell. Biochem. 300, 249-258.

Lv J., Liu H., Wang Q., Tang Z., Hou L. and Zhang B. (2003). Molecular cloning of a novel human gene encoding histone acetyltransferase-like protein involved in transcriptional activation of hTERT. Biochem. Biophys. Res. Commun. 311, 506-513.

Ma N., Liu H., Wu Y., Yao M. and Zhang B. (2022). Inhibition of N-acetyltransferase 10 suppresses the progression of prostate cancer through regulation of DNA replication. Int. J. Mol. Sci. 23, 6573.

Qi P., Chen Y.K., Cui R.L., Heng R.J., Xu S., He X.Y., Yue A.M., Kang J.K., Li H.H., Zhu Y.X., Wang C., Chen Y.L., Hu K., Yin Y.Y., Xuan L.X. and Song Y. (2022). Overexpression of NAT10 induced platinum drugs resistance in breast cancer cell. Zhonghua Zhong Liu Za Zhi. 44, 540-549 (in Chinese).

Shen Q., Zheng X., McNutt M.A., Guang L., Sun Y., Wang J., Gong Y., Hou L. and Zhang B. (2009). NAT10, a nucleolar protein, localizes to the midbody and regulates cytokinesis and acetylation of microtubules. Exp. Cell Res. 315, 1653-1667.

Tan Y., Zheng J., Liu X., Lu M., Zhang C., Xing B. and Du X. (2018). Loss of nucleolar localization of NAT10 promotes cell migration and invasion in hepatocellular carcinoma. Biochem Biophys Res. Commun. 499, 1032-1038.

Tao W., Tian G., Xu S., Li J., Zhang Z. and Li J. (2021). NAT10 as a potential prognostic biomarker and therapeutic target for HNSCC. Cancer Cell Int. 21, 413.

Wang Z., Huang Y., Lu W., Liu J., Li X., Zhu S., Liu H. and Song Y. (2022a). c-myc-mediated upregulation of NAT10 facilitates tumor development via cell cycle regulation in non-small cell lung cancer. Med. Oncol. 39, 140.

Wang G., Zhang M., Zhang Y., Xie Y., Zou J., Zhong J., Zheng Z., Zhou X., Zheng Y., Chen B. and Liu C. (2022b). NAT10-mediated mRNA N4-acetylcytidine modification promotes bladder cancer progression. Clin. Transl. Med. 12, e738.

Wu J., Zhu H., Wu J., Chen W. and Guan X. (2018). Inhibition of N-acetyltransferase 10 using remodelin attenuates doxorubicin resistance by reversing the epithelial-mesenchymal transition in breast cancer. Am. J. Transl. Res. 10, 256-264.

Zhang Z.X., Zhang W.N., Sun Y.Y., Li Y.H., Xu Z.M. and Fu W.N. (2018). CREB promotes laryngeal cancer cell migration via MYCT1/NAT10 axis. OncoTargets Ther. 11, 1323-1331.

Zhang X., Chen J., Jiang S., He S., Bai Y., Zhu L., Ma R. and Liang X. (2019). N-acetyltransferase 10 enhances doxorubicin resistance in human hepatocellular carcinoma cell lines by promoting the Epithelial-to-Mesenchymal transition. Oxid. Med. Cell. Longev. 2019, 7561879.

Zi J., Han Q., Gu S., McGrath M., Kane S., Song C. and Ge Z. (2020). Targeting NAT10 Induces apoptosis associated with enhancing endoplasmic reticulum stress in acute myeloid leukemia cells. Front. Oncol. 10, 598107.

Accepted April 22, 2024